Supporting Information

Revealing the role of unique local structure in lanthanide-doped $Cs_2LiInCl_6$ for boosting visible and NIR-II luminescence

Qiudong Duan,[a] Yusheng Xu,[a] Ruijing Yang,[a] Dongfeng Hong,[a] Dacheng Zhou,[a, b] Qi Wang,[a, b] Yong Yang,[a, b] Jin Han, [a, b] Yugeng Wen*[a, b] and Jianbei Qiu*[a, b]

[a] Faculty of Material Science and Engineering, Kunming University of Science and Technology, Kunming 650093, China

[b] Key Lab of Advanced Materials of Yunnan Province, Kunming 650093, China

* Corresponding authors

Yugeng Wen: E-mail address: wenyg@kust.edu.cn

Jianbei Qiu: E-mail address: qiu@kust.edu.cn

Experimental section

Materials synthesis

The $Cs_2LiInCl_6$ double perovskites were synthesized using a solid-state reaction method. To synthesize Er^{3+} -Yb^{3+} co-doped $Cs_2LiInCl_6$ DPs, stoichiometric amounts of

CsCl (Aladdin 99.9%), LiCl (Aladdin 99%), $InCl_3 \cdot 4H_2O$ (Aladdin 99.9%), $ErCl_3 \cdot 6H_2O$ (Aladdin 99.99%) and $YbCl_3 \cdot 6H_2O$ (Aladdin 99.99%) were thoroughly mixed by grinding in an agate mortar, with a small amount of deionized water as the wetting agent for 30 min, until the powder was uniform. All the chemicals were used as received without further purification. The powder was then transferred to an alumina crucible, covered with a lid, sintered in air at 350°C for 2 h, and was finally cooled down to room temperature slowly.

Characterization

The powder XRD patterns were identified using a laboratory powder XRD system at a scanning rate of 5° min^{-1} in the 2θ range from 10° to 60°, with Cu Kα radiation (λ=0.15418 nm) at 40 kV and 40 mA. The morphological images of the samples were recorded by SEM (TESCAN MIRA LMS, Czechia), and energy-dispersive spectrometry (EDS) spectroscopy on a Hitachi S-3500N scanning electron microscope, operated at 200 kV with a resolution of 102 eV. Raman spectra were recorded using LabRAM HR Evolution (HORIBA, France). Absorption spectra were recorded using UV-3600 (SPC, Japan). Thermogravimetric analysis (TGA) data were recorded using a TGA-4000 (PerkinElmer, USA) instrument. The samples were heated in the range of 303–1073 K at a heating rate of 10℃/min under an N_2 atmosphere. The photoluminescence was investigated using a Pro-FL spectrophotometer (F-7000, Hitachi, Japan), and the spectrometer (FLS980, Edinburgh, United Kingdom) equipped with modulated 980 nm and 1550 nm continuous wavelength laser as the pump sources, respectively.

First-principles calculations

The Vienna Ab initio Simulation Package (VASP) were used to perform first-principles density functional theory (DFT) calculations on the material. The projector augmented wave (PAW) and Perdew-Burke-Ernzerhof (PBE) methodologies were employed with the computational efficiency of pseudopotential DFT algorithms. We use a plane wave cutoff energy of 350 eV, an energy convergence standard value of 10^{-5}, an atomic force standard of 0.02, and an optimized *k*-point setting of (111). The *k* points with self-consistent method of $Cs_2LiInCl_6$ and $Cs_2NaInCl_6$ are set to (332) and (233),

respectively. After structural optimization and self-consistency of the material matrix, the band structure and density of states (DOS) are obtained. The symmetry change is obtained by structural optimization of rare earth doped materials.

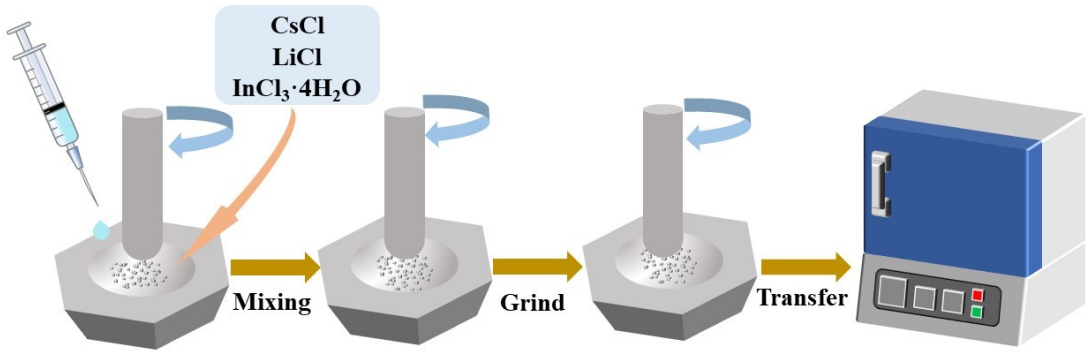

Fig. S1 The schematic diagram of the synthesis process of $Cs_2LiInCl_6$.

Table S1 Inductively coupled plasma optical emission spectrometer (ICP-OES) data of $Cs_2LiInCl_6$:18%Yb^{3+}, 5%Er^{3+} and $Cs_2LiInCl_6$:15%Yb^{3+}, 2%Er^{3+}.

Sample	Precursor		Product	
	Er/%	Yb/%	Er/%	Yb/%
$Cs_2LiInCl_6$	2	15	0	24
$Cs_2LiInCl_6$	5	18	6	25

(a)

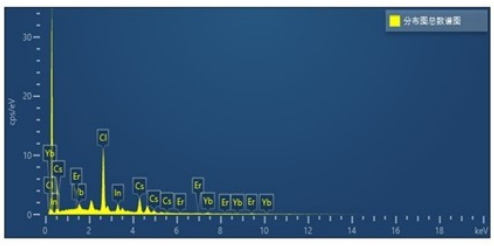

Element	At%
Cs	23.80
In	8.63
Cl	64.15
Yb	2.85
Er	0.57
Gross	100

(b)

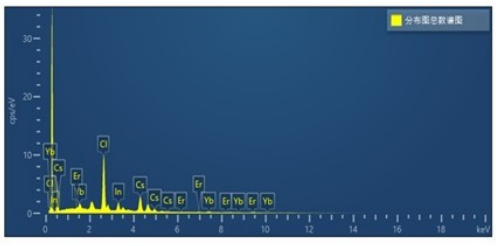

Element	At%
Cs	25.56
In	9.24
Cl	60.48
Yb	3.35
Er	1.36
Gross	100

Fig. S2 The results of energy dispersive X-ray (EDX) measurements for $Cs_2LiInCl_6$:18%Yb^{3+}, 5%Er^{3+} and $Cs_2LiInCl_6$:15%Yb^{3+}, 2%Er^{3+}.

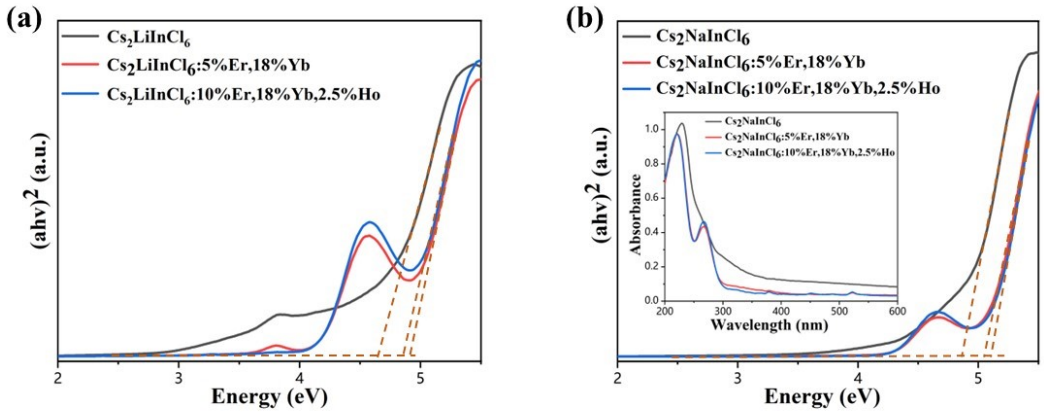

Fig. S3 The linear portion of the photon energy axis for (a) $Cs_2LiInCl_6$, $Cs_2LiInCl_6$:18%Yb^{3+}, 10%Er^{3+}, 2.5%Ho^{3+} and $Cs_2LiInCl_6$:18%Yb^{3+}, 5%Er^{3+}. And (b) $Cs_2NaInCl_6$, $Cs_2NaInCl_6$:18%Yb^{3+}, 10%Er^{3+}, 2.5%Ho^{3+} and $Cs_2NaInCl_6$:18%Yb^{3+}, 5%Er^{3+}. The inset shows the corresponding absorption spectra of $Cs_2NaInCl_6$-based samples.

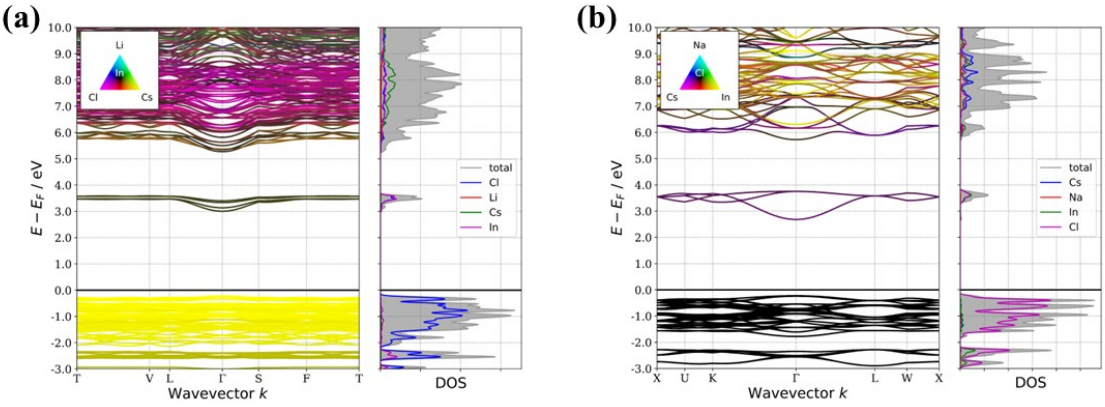

Fig. S4 Calculated band structures and DOS of (a) $Cs_2LiInCl_6$ and (b) $Cs_2NaInCl_6$ with the first-principles method.

Table S2 The fitting results of PL decay time for $Cs_2LiInCl_6$:18%Yb^{3+}, 5%Er^{3+} and $Cs_2NaInCl_6$:18%Yb^{3+}, 5%Er^{3+} at 552 nm under 980 nm excitation.

	τ_1(s)	τ_2(s)	τ_3(s)	B_1	B_2	B_3	Wavelength(nm)
$Cs_2LiInCl_6$	**2.730E-3**	--	--	**1.835E+3**	--	--	**552**
$Cs_2NaInCl_6$	**6.689E-4**	**2.541E-3**	**8.547E-3**	**8.199E+2**	**8.998E+2**	**1.581E+2**	

Table S3 The fitting results of PL decay time for $Cs_2LiInCl_6$:18%Yb^{3+}, 5%Er^{3+} and $Cs_2NaInCl_6$:18%Yb^{3+}, 5%Er^{3+} at 1540 nm under 980 nm excitation.

	τ_1(s)	τ_2(s)	τ_3(s)	B_1	B_2	B_3	Wavelength(nm)
$Cs_2LiInCl_6$	1.760E-2	--	--	4.245E+3	--	--	1540
$Cs_2NaInCl_6$	3.352E-3	1.066E-2	--	1.545E+3	3.033E+3	--	

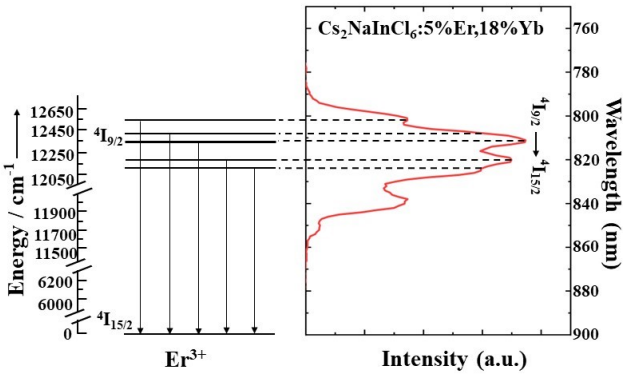

Fig. S5 The energy level splitting of $Cs_2NaInCl_6$:18%Yb^{3+}, 5%Er^{3+} from the $^4I_{9/2}$ crystal field.

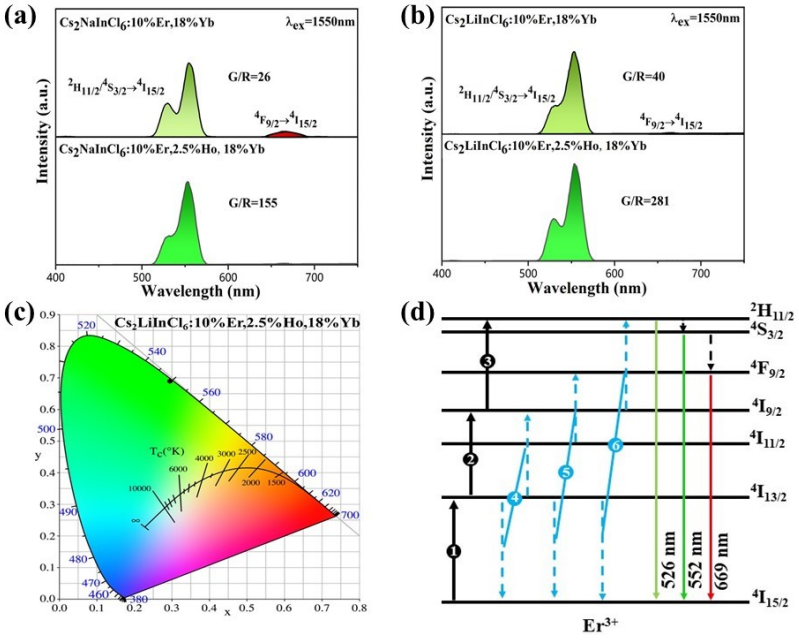

Fig. S6 PL spectra for (a) $Cs_2NaInCl_6$ and (b) $Cs_2LiInCl_6$ with different concentrations under 1550 nm excitation. (c) CIE chromaticity coordinate of $Cs_2LiInCl_6$:18%Yb^{3+}, 10%Er^{3+}, 2.5%Ho^{3+} under 1550 nm excitation. (d) UC luminescence populating mechanism of $Cs_2LiInCl_6$: Yb^{3+}, Er^{3+} under 1550 nm excitation.

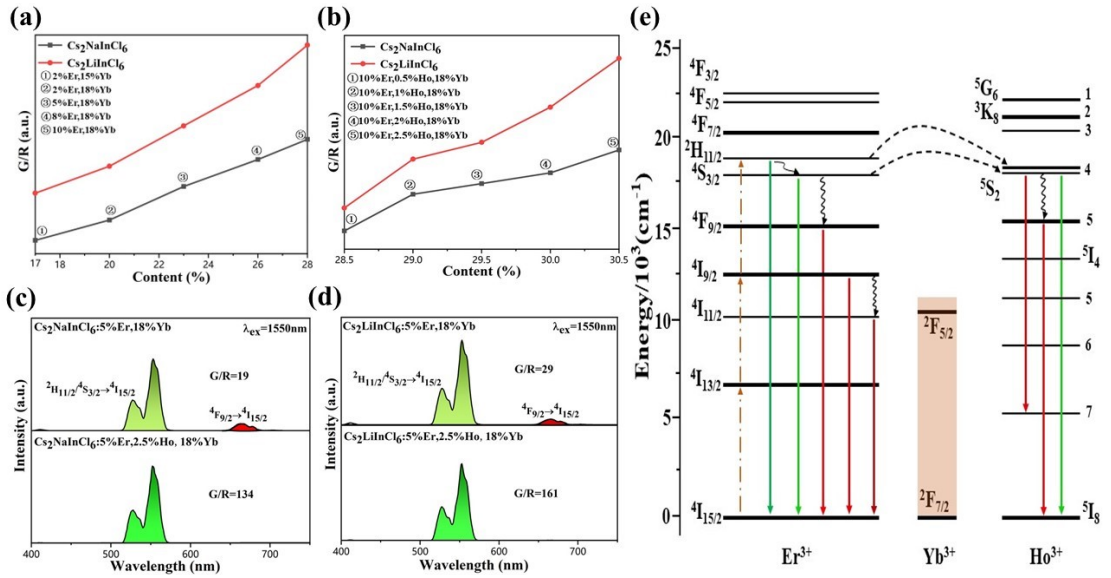

Fig. S7 The green-to-red ratio (G/R) for $Cs_2LiInCl_6$ and $Cs_2NaInCl_6$ with different (a) Yb^{3+}-Er^{3+} co-doping and (b) Yb^{3+}, Er^{3+}, Ho^{3+} tri-doping concentrations under 1550 nm excitation. PL spectra for (a) $Cs_2NaInCl_6$ and (b) $Cs_2LiInCl_6$ with the same co-doing and tri-doping concentrations under 1550 nm excitation. (e) UC luminescence populating mechanism of $Cs_2LiInCl_6$: Yb^{3+}, Er^{3+}, Ho^{3+} under 1550 nm excitation.

Note: Two reasons are responsible for the large enhancement of the green-to-red ratio in $Cs_2LiInCl_6$:Yb^{3+}, Er^{3+}, Ho^{3+} compared with $Cs_2LiInCl_6$:Yb^{3+}, Er^{3+}. One is that the energy levels of Ho^{3+} match very well with those of Er^{3+} for green emissions, and the three-photon process would occur under 1550 nm excitation, thus increasing the $^2H_{11/2}$ and $^4S_{3/2}$ transitions of Er^{3+}. Meanwhile, energy can also be efficiently transferred from the $^4S_{3/2}$ level of Er^{3+} to the $^5S_2$ level of Ho^{3+}, further enhancing the green emissions. Another reason is due to very weak electron-phonon coupling in the $Cs_2LiInCl_6$ host, nonradiative relaxation from $^4S_{3/2}$ to $^4F_{9/2}$ of Er^{3+} and $^5S_2$ to $^5F_5$ of Ho^{3+} can rarely occur, leading to the largely suppressed red emissions for both Er^{3+} and Ho^{3+}. The increased green emission and decreased red emission thus would further enlarge the green-to-red ratio after doping with Ho^{3+}.

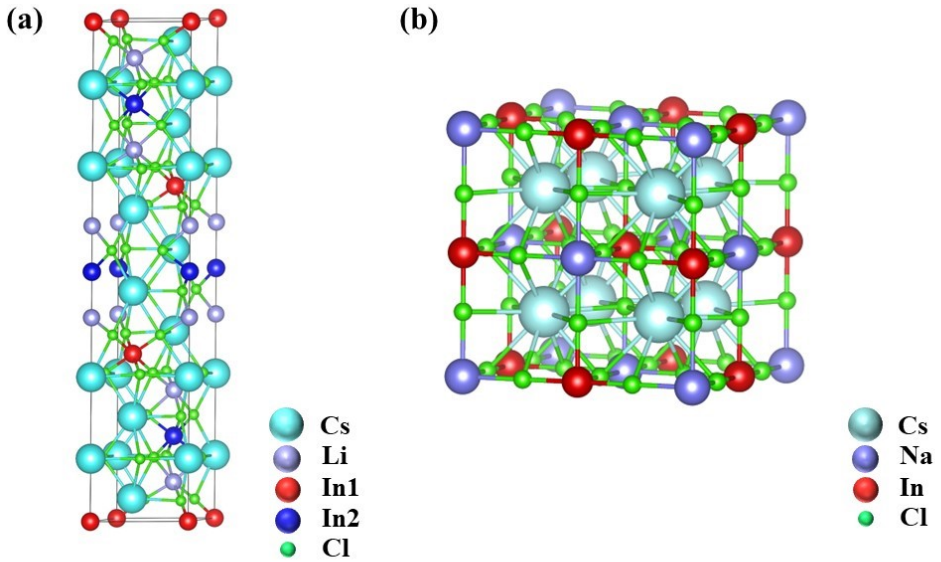

Fig. S8 The crystalline structure of (a) $Cs_2LiInCl_6$ and (b) $Cs_2NaInCl_6$ in a single unit cell.

Note: In a single unit cell of $Cs_2LiInCl_6$, the total In sites are 16, of which are 10 In1 sites and 6 In2 sites. Therefore, the occupancy of In1 is 5/8, and the occupancy of In2 is 3/8. Whereas the occupancy of $Cs_2NaInCl_6$ is 1 for In site, due to its cubic-phase structure. Only considering the case of Er^{3+}-doped $Cs_2LiInCl_6$, at low doping concentration, two or more Er^{3+} ions may occupy the same In sites (In1 or In2), thus it does not make sense statistically. However, at high doping concentrations, as the number of Er^{3+} ions increase, the occupancy ratio of In1/In2 should be close to 5/3, indicating that the statistical distribution of Er^{3+} ions can be more meaningful and accurate. In particular, the distances of In1–In1 (or In2–In2) and In1–In2 are 7.3184 and 7.3712 Å, respectively, leading to increased distance of two adjacent of Er^{3+} ions in $Cs_2LiInCl_6$, blocking the cross-relaxation process at a high doping level of Er^{3+}.